Int. J. Electrochem. Sci., 10 **(2015)** 2355 - 2369

International Journal of
ELECTROCHEMICAL
SCIENCE
www.electrochemsci.org

Electrooxidation Kinetics of Hydrazine on Y-type Zeolite-encapsulated Ni(II)(salen) Complex Supported on Graphite Modified Electrode

Rong Zhang[1,*], *Lu Liu*[1], *Yuehua Li*[1] , *Wenyang Wang*[1,2], *and Ruifeng Li*[1,2]

[1] College of Chemistry and Chemical Engineering, Taiyuan University of Technology, Taiyuan, 030024, China
[2] Key Laboratory of Coal Science and Technology, MOE, Taiyuan University of Technology, Taiyuan, 030024, China
[*]E-mail: zhangrong@tyut.edu.cn

Received: 14 December 2014 / *Accepted:* 30 December 2014 / *Published:* 19 January 2015

The electrocatalytic oxidation of hydrazine was investigated on the zeolite-encapsulated Ni(II)(salen) [salen: N, N'-bis(salicylidene)ethylenediamine] complex supported on graphite modified glassy carbon electrode (Ni(II)(salen)Y/GCE). The modified electrode shows efficient electrocatalytic activity for anodic oxidation of hydrazine in 1.0 M NaOH solution. Anodic peak potential of hydrazine oxidation at the surface of Ni(II)(salen)Y/GCE shifts near 100 mV toward negative position compared with that on bare GCE. And the Ni(II)(salen)Y/GCE also significantly enhances the anodic current for catalytic oxidation of hydrazine compared with that on bare GCE, Graphite/GCE, NaY/GCE and Ni(II)Y/GCE. The kinetics of the reaction between the Ni(II)(salen) complex on the surface of modified electrode and hydrazine was characterized using cyclic voltammetry and chronoamperometry. The diffusion coefficient (D) and electron transfer coefficient (α) of hydrazine under the experimental conditions were investigated, and the heterogeneous rate constant, k_{cat}, for the oxidation of hydrazine at the surface of the Ni(II)(salen)Y modified electrode was also obtained in the same time. Finally, the general reaction mechanism for the electrooxidation of hydrazine on the Ni(II)(salen)Y/GCE in pH 14 alkaline solutions involves a transfer of four electrons process in which the first electron transfer reaction acts as the rate-limiting step followed by a 3-electron process generating environmentally friendly nitrogen and water as final products.

Keywords: Y-type zeolite-encapsulated Ni(II)(salen); Zeolite-Modified electrode; Electrocatalytic oxidation hydrazine; Mechanism

1. INTRODUCTION

Hydrazine (N_2H_4) is an important high-performance fuel in aerospace propulsion applications, which also impresses promising potential applications in fuel cells. In fact, hydrazine may be an ideal

fuel for a direct fuel cell system because the absence of carbon atoms in hydrazine leads to zero production of species that may poison the electrocatalysts and reduces the overall emission of greenhouse gases (CO_2). Hydrazine is also a hydrogen-rich fuel with high hydrogen content 12.5 wt.%. Its hydrogen storage capability is higher than that of sodium borohydride (10.6 wt.%) and equivalent to that of methanol. The direct hydrazine fuel cell (DHFC) demonstrates a higher electromotive force of 1.56 V [1], which is higher for DHFCs than that for other fuel cells using hydrogen (1.24 V) or methanol (1.19 V) as a fuel. In addition, the decomposition products of hydrazine, nitrogen and water, are ecologically friendly. Although hydrazine is highly toxic and carcinogenic compound [2], it is an ideal fuel for direct liquid-feed fuel cells given that hydrazine oxidation only generates environmentally friendly nitrogen and water so as to not produce species which can poison the electrocatalysts. Hydrazine as a fuel for alkaline fuel cells has been studied since the 1970s [3]. But only in recent years there have been increased research efforts in this field owing to the increased cost of oil and growing demand for stationary and mobile applications. Furthermore, to the best of our knowledge the kinetics and mechanism of hydrazine oxidation, in particular those operating on the non-platinum catalysts, is still uncertain. The mechanism of hydrazine oxidation in alkaline media on polycrystalline and single-crystal surfaces of platinum was studied by voltammetry and on-line electrochemical mass spectrometry [4]. This research showed that hydrazine oxidation at platinum electrodes is a diffusion-controlled electrocatalytic mechanism over a wide potential region. The kinetics at low overpotentials indicates that hydrazine oxidation on the surfaces of Pt (110) and Pt (111) is limited by electrochemical steps, whereas on Pt (100), the chemical step that involves a N_2H_2 intermediate is a likely rate-determining step. Study on the hydrazine oxidation mechanism that operate in alkaline media on the other kinds of catalysts is relatively little at present. With similar activity to Pt-based catalysts, these catalysts are significantly cheaper.

It has been determined from a review in 2010 [5] and others in recent years that noble metals are highly active for the oxidation of hydrazine, such as Au [6-10], Ag [11], Pt [13-16, 20] and Pd[17-19], but the use of them as an electrode material in direct hydrazine fuel cells is limited by their high price. Accordingly, there are some other kinds of catalysts used for hydrazine oxidation, for example, organic phenol derivatives [21-23] and transition metal macrocyclic complexes [24-28]. These transition metal macrocyclic complexes possess redox behavior with easier operation than the corresponding center transition metal ions. Considering that the nickel macrocyclic complexes can be easily electropolymerized onto an electrode surface in the alkaline solution to form modified electrode, Zheng and Song [24] prepared nickel(II)–baicalein complex (Ni(II)-BA) modified multiwall carbon nanotube paste electrode (Ni(II)-BA-MWCNT-PE) by electrodepositing Ni(II)-BA complex on the surface of MWCNT-PE in alkaline solution and investigated its electrocatalytic activity and kinetic behavior toward the oxidation of hydrazine. Also, poly(Ni(II)(teta)) modified glassy carbon electrode [25], cobalt(II) bis (benzoylacetone) ethylenediimino multiwall carbon nanotube-modified carbon paste electrode [27] and Mn(II)-(pyterpy)complex/MWNTs-modified GC electrode[28] were employed for studying the electrocatalytic oxidation of hydrazine in 0.1M NaOH solution. Although these modified electrodes exhibit efficient electrocatalytic activities toward oxidation of hydrazine, they can only be used for the application of hydrazine determination in environmental water rather than fuel cells because of their poor mechanical and thermal stability. In order to retain the transition

metal complexes' high electroactivities as well as good chemical and thermal stability, different matrices have been used for the immobilization of the metal complexes. Among these, inorganic nanostructured materials are more promising because of their regular structure and high active surface area, e.g., zeolite was employed as a dispersion medium for primary catalysts of different reactions [29-30, 37, 39].

Zeolite-modified electrodes (ZMEs), a sub-category of the chemically modified electrodes (CMEs), were largely studied and applied in electrocatalysis, sensors [31-33]. Ni-containing zeolites [34], Pt-and Pt-Ru-zeolites [35], Ti-zeolites [36] have been used for catalytic purpose. Compared with transition metals-zeolite, transition metal complexes of Schiff-base supported into zeolite showed more prominent electrochemical quality [29-30]. In this work, we prepared NaY zeolite-encapsulated Ni(II)(salen) [salen: N, N'-bis(salicylidene)ethylenediamine] complex modified electrodes and studied on their inherent electrochemical behaviors and used them to evaluate the electrocatalytic performance of hydrazine oxidation in the alkaline solution. The reaction mechanism of hydrazine oxidation on these modified electrodes (named as Ni(II)(salen)Y/GCEs) in alkaline medium was further investigated using cyclic voltammetry and chronoamperometry. The kinetic parameters of hydrazine oxidation at the surface of Ni(II)(salen)Y/GCEs were obtained from the electrochemical experiments.

2. EXPERIMENTAL

2.1. Reagents and chemicals

NaOH aqueous solution (1.0 M) for electrochemical experiments was prepared using doubly deionized water. $Ni(OAc)_2 \cdot 2H_2O$, hydrazine (N_2H_4), and other compounds of analytical grade were commercially available and used as received without further purification. NaY with its ratio of 5.80 for SiO_2/Al_2O_3 was from Fushun Research Institute of Petroleum and Petrochemicals, the China Petroleum and Chemical Corporation.

2.2. Preparation of Ni(II)(salen)Y and its modified electrode

Ni(II)Y zeolite was obtained by subjecting NaY zeolite to ion-exchange in water solutions (0.01 M) of nickel acetate at room temperature two times (24 h for each time), followed by washing and drying. Ni(II)(salen) complex inside the faujasite structure was synthesized through the reaction between Ni(II)Y and salen ligand by flexible ligand method [37]. The typical procedures refer to our previous report [30]

Prior to preparation of the modified electrode of catalyst, the GC electrode was polished to a mirror-like surface with slurry of alumina and water on polishing cloth and rinsed with doubly distilled water. Then, it was cleaned ultrasonically in acetone, absolute ethanol, HNO_3-H_2O (1:1, v/v) solution and distilled water in succession, then dried in air before use. The modified electrode was prepared according to our previous work [29]. Typically, 30 mg of Ni(II)(salen)Y and 30 mg of high purity graphite were dispersed in 1 ml of tetrahydrofuran (THF) ultrasonically to form a black suspension.

Four microliters of this black suspension was pipetted directly on the freshly polished surface of glassy carbon electrode (GCE), forming Ni(II)(salen)Y composite film. Dried subsequently in air at room temperature for approximately 1 h, the composite film was further coated by 10 μl of polystyrene solution in THF (8 g/l) and then dried overnight at room temperature. Thus, the Ni(II)(Salen)Y modified electrode was obtained. Similarly, the Ni(II)Y/GC and NaY/GC modified electrodes were obtained by replacing Ni(II)(salen)Y with Ni(II)Y and NaY zeolite. The Graphite/GCE was prepared using only high purity graphite as the modifier by above approach. The Ni(II)(salen)Y/GCE, Ni(II)Y/GCE, NaY/GCE, Graphite/GCE and bare GCE were all used as working electrode in electrochemical experiments.

2.3. Apparatus and Procedures

Electrochemical measurements were carried out in a one-compartment cell using CHI660E electrochemical workstation from Chenhua Instrument Co., Shanghai, China. Teflon shrouded glassy carbon electrodes (GCEs) (geometric area, 0.0707 cm^2) and their modified GCEs by the NaY, Ni(II)Y, Ni(II)(salen)Y and graphite samples were used as working electrodes. Pt plate (2 mm×7 mm) served as auxiliary electrode and the potentials were reported against a saturated calomel electrode (SCE). Electrochemical experiments were performed using 1.0 M NaOH solution as the supporting electrolyte. High purity N_2 regulated by a flow-meter (equipped with needle valves) was used to deoxygenate the measurement cell. The electrolyte solution was purged with highly purified nitrogen for approximately 15 min before experiments. A nitrogen environment was then kept over solutions in the cell during all experiments of electrochemical and electrocatalytic hydrazine oxidation. All experiments were conducted at ambient temperature of 22±1 ˚C.

3. RESULTS AND DISCUSSION

3.1. Characterization and electrochemical behavior of Ni(II)(salen)Y

Fig.1 (A) shows the FT-IR spectra of Ni(II)(salen)Y and NaY. As can be observed, the range of 450-1200 cm^{-1} is dominated by the framework vibrations of zeolite Y for NaY and Ni(II)(salen)Y. And the band at 1640 cm^{-1}, due to the bending vibration of H_2O in zeolite lattice, is also observed in all two spectra. In addition, the bands attributed to aromatic and C=N vibrations of the salen ligand are present at about 1260-1520 cm^{-1} in the IR spectra of the Ni(II)(salen)Y samples [37-39]. Also, the weak bands at 2938 and 2984 cm^{-1} ascribed to the stretching vibrations of the -CH_2- in salen ligand are seen for Ni(II)(salen)Y. In contrast, these bands are absent in the spectra of NaY sample. This gives one piece of effective evidence for the presence of Ni(II)(salen) complex into NaY zeolite. The XRD patterns of NaY and Ni(II)(salen)Y samples are shown in Fig.1(B). It is observed that the XRD pattern of Ni(II)(salen)Y reflects the topological structure of Y type zeolite despite a slight decline in crystallinity of NaY, suggesting that the formation of Ni(II)(salen) complex inside the faujasite structure of NaY

zeolite by flexible ligand method in the synthesis process does not greatly affect the crystallization of NaY zeolite and the crystal structure of Y zeolite is intact.

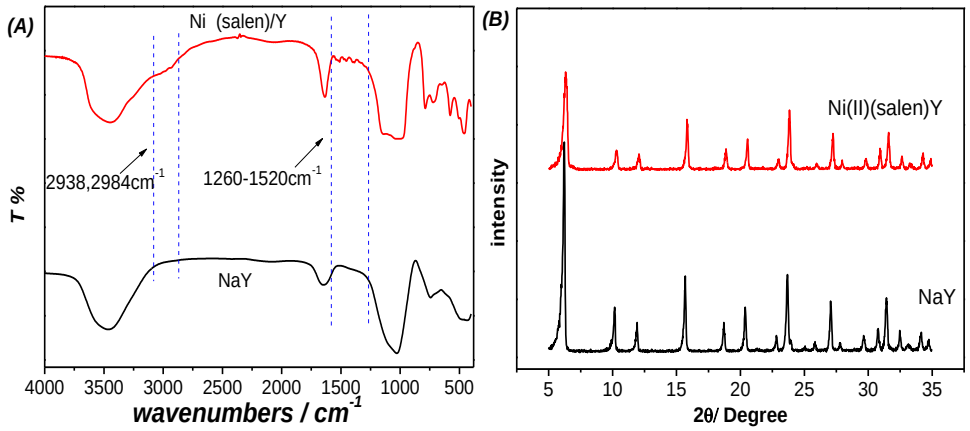

Figure 1. FT-IR Spectra (A) and XRD patterns (B) of Ni(II)(Salen)Y and NaY

The electrochemical behavior of Ni(II)(salen)Y/GCE was investigated by cyclic voltammetry. Fig. 2 (A) shows cyclic voltammograms of the Ni(II)(salen)Y/GCE, Ni(II)Y/GCE and bare/GCE in 1.0 M NaOH solution at a scan rate of 50 mV s^{-1}. At bare GCE, there is no electrochemical response observed in the alkali solution, while at Ni(II)(salen)Y/GCE, a pair of well-defined redox peaks with large peak current response (i_{pc}=23.5μA) and small peak potential separation (about ΔE_p=70 mV) are observed. However, at Ni(II)Y/GCE, the current response is smaller (i_{pc}=8.5 μA) and the peak potential separation is larger (about ΔE_p=105 mV). These results indicate that the anodic and cathodic peaks observed are from the redox couple of Ni(III)/Ni(II) on the surface of the modified electrode in the alkali solution[24]. Also, the formal potential of the redox couple on Ni(II)(salen)Y/GCE shifts to less positive potential ($E^{0'}$=0.355 V) compared with that ($E^{0'}$=0.381 V) on Ni(II)Y/GCE. These results indicate that the electrochemical reversibility and electrochemical response on the Ni(II)(salen)Y/GCE are improved with respect to those on Ni(II)Y/GCE. This might result from the fact that the Schiff-base, salen, acts as ligand for immobilizing both the reduction state, Ni(II), and the oxidation state, Ni(III). The redox process of the Ni(II)(salen)Y modified electrode is expressed as follows:

$$Ni(II)(OH)_2(salen)+OH^- \underset{+e^-}{\overset{-e^-}{\rightleftharpoons}} Ni(III)(OOH)(salen)+H_2O \quad (1)$$

Fig.2 (B) shows cyclic voltammograms of Ni(II)(salen)Y/GCE in pH 11, 12, 13 and 14 alkaline solutions. The inset gives the formal potentials ($E^{0'}$) and the anodic peak currents (i_{pa}) of Ni(II)(salen)Y/GCE in different pH alkaline electrolytes versus pH value. The formal potentials shift to less positive potential and the anodic peak currents are enhanced with the increase of pH value of the solution, further indicating that OH^- participates in the redox process of the modified electrode as shown in the reaction equation (1). And the pH 14 NaOH solution in which the reversibility and the electrochemical response are improved for the modified electrode was used as the supporting electrolyte in the following electrochemical experiments.

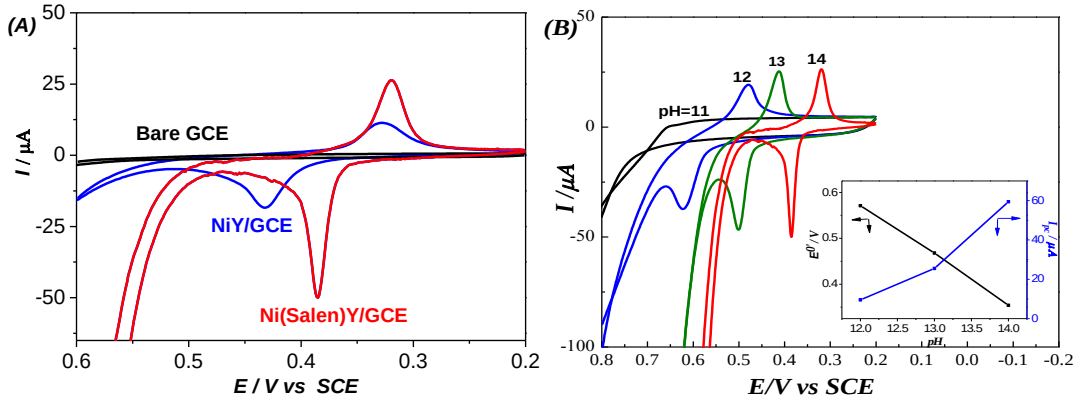

Figure 2. (A) Cyclic voltammograms of Ni(II)(salen)Y/GCE, Ni(II)Y/GCE and bare GCE in 1.0 M NaOH solution at scan rate of 50 mV s^{-1}; (B) Cyclic voltammograms of Ni(II)(salen)Y/GCE in alkaline solutions of pH=11, 12, 13 and 14 at scan rate of 20 mV s^{-1}. Inset: Dependence of $E^{0'}$ and i_{pa} on pH

The influence of scan rate in a wide range from 1 to 3000 mV s^{-1} on the electrochemical behavior of Ni(II)(salen)Y/GCE was investigated in 1.0 M NaOH solution (Fig.3). As shown in inset (a) of Fig.3, the linear dependence of the peak current on the potential scan rate below 100 mVs^{-1} indicates that the nature of the redox process of Ni(III)(OOH)(salen)/Ni(II)$(OH)_2$(salen) on the modified electrode is a surface-confined redox process. Inset (b) exhibits the variation of the peak potential with the logarithm of the potential scan rate. It is seen from inset (b) that the potential separation is almost independent of the v at lower potential scan rate. But, at higher potential scan rates, the potential separation increases with the increase of potential scan rate, indicating the limitation arising from the charge transfer kinetics [21, 22]. When the scan rate v>1.0 Vs^{-1}, the peak potentials become proportional to the logarithm of the scan rate (inset (c)). Based on the procedure of Laviron, if the value of $n\Delta E_p > 0.2V$, it is possible to determinate the electron transfer coefficient, α, from the slope of variation of E_p=f(log$v$). In fact, a graph of E_p=f(log$v$) yields two straight lines with a slope equal to 2.303RT/2$(1-\alpha)nF$ for anodic peak and -2.303RT/2αnF for cathodic peak (inset (c)). The calculated value of α is 0.67. According to the equation (2),

$$\log k_s = \alpha\log(1-\alpha) + (1-\alpha)\log\alpha - \log\frac{RT}{nF\nu} - \frac{\alpha(1-\alpha)nF\Delta E_p}{2.3RT} \qquad (2)$$

the apparent rate constant of electrode reaction, k_s, is calculated to be 7.74 s^{-1} when v =3.0 Vs^{-1} (ΔE_p=0.214 V s^{-1}). The obtained k_s value is higher than that for some modifiers in the literatures (1.5 s^{-1}[27], 2.21 s^{-1}[24], 4.44 s^{-1}[23]) but lower than that for benzofuran derivative in modified electrode-based CNT-ionic liquids obtained in the literature [21] (11.0±0.1 s^{-1}).

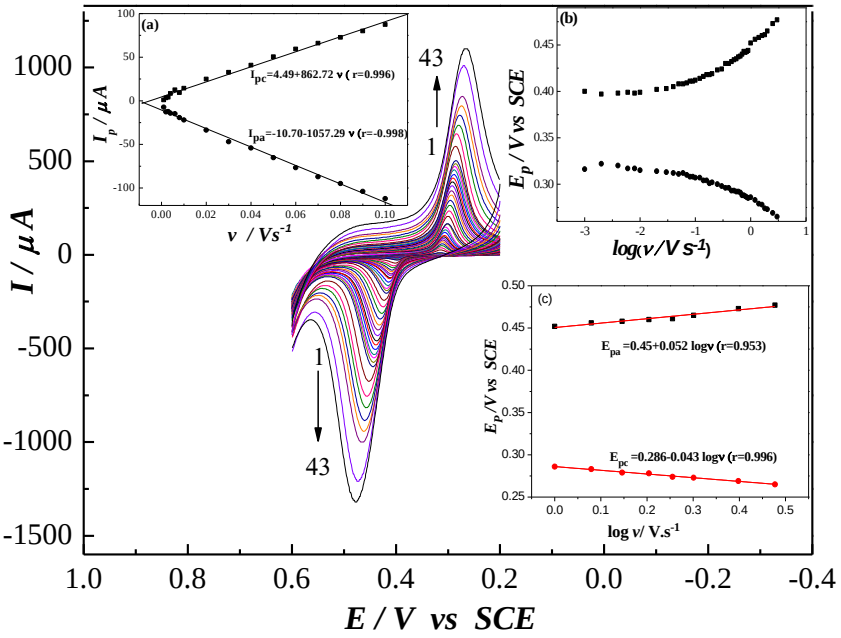

Figure 3. cyclic voltammograms of Ni(II)(Salen)Y/GCE in 1.0 M NaOH solution at scan rate from 1 to 3000 mVs^{-1}. Inset: (a) plots of peak current vs potential scan rate below 0.1 Vs^{-1}; (b) variation of peak potential vs logarithm of the potential scan rate; and (c) the linearity part of plot inset (b) for the higher potential scan rate.

3.2. Electrocatalytical activity of Ni(II)(salen)Y/GCE for oxidation of hydrazine

In order to test the electrocatalytic performance of Ni(II)(salen)Y modified electrode for hydrazine oxidation, the cyclic voltammetric responses of Bare GCE, Graphite/GCE, NaY/GCE, Ni(II)Y/GCE and Ni(II)(salen)Y/GCE were obtained in the absence and presence of 0.075 M hydrazine in 1.0 M NaOH solution, as shown in Fig. 4. It can be seen that there are no electrochemical responses on bare GCE, Graphite/GCE and NaY/GCE in the absence of hydrazine solution, while there is a pair of redox peaks corresponding to the Ni(III)(OOH)/Ni(II)$(OH)_2$ couple (Fig.4 (D) g) for Ni(II)Y/GCE and to Ni(III)(OOH)(salen)/Ni(II)$(OH)_2$(salen) couple (Fig.4 (E) i) for Ni(II)(salen)Y/GCE in the absence of hydrazine. In the presence of hydrazine, no well-defined anodic peak is observed on Ni(II)Y modified electrode despite an anodic current increase. While a noticeable anodic wave with a peak potential of 0.499 V and a significantly large current appears on the Ni(II)(salen)/Y in the alkaline solution containing 0.075M hydrazine. Obviously, the so large catalytic current of hydrazine oxidation on Ni(salen)Y/GCE results from the Ni(Salen) not the Ni^{+2}. Furthermore, as it will be discussed below, this anodic peak current increases linearly with the concentration of hydrazine on the Ni(II)(salen)/Y, suggesting that this is the region of potential in which the hydrazine is involved in the oxidation process. At the reverse scan, no reduction peak is observed, but the hydrazine is still oxidized and as a result a new peak at 0.450 V can be observed on the Ni(II)(salen)/Y. These results indicate that Ni(II)(salen) complex as a mediator of the electron transfer plays an effective role in hydrazine oxidation process. Maybe it is the site isolation effect of Y zeolite [37, 39] that prevents from the dimerization and then deactivation of the Ni(II)(salen)

complexes in the NaY for catalytic oxidation hydrazine. This is potentially a part of reasons for effectively elctrocatalytic oxidation performance of Ni(II)(salen)Y. In addition, from the CV shape of hydrazine oxidation on the Ni(II)(salen)Y modified electrode, an electrocatalytic behavior of the hydrazine oxidation is observed at the surface of Ni(II)(salen)Y/GCE via an EC' catalytic mechanism. This mechanism is shown in scheme 1. That is, as shown in the chemical reaction (C'), hydrazine is oxidized by the Ni(III)(OOH)(salen) which is produced via an electrochemical reaction (E).

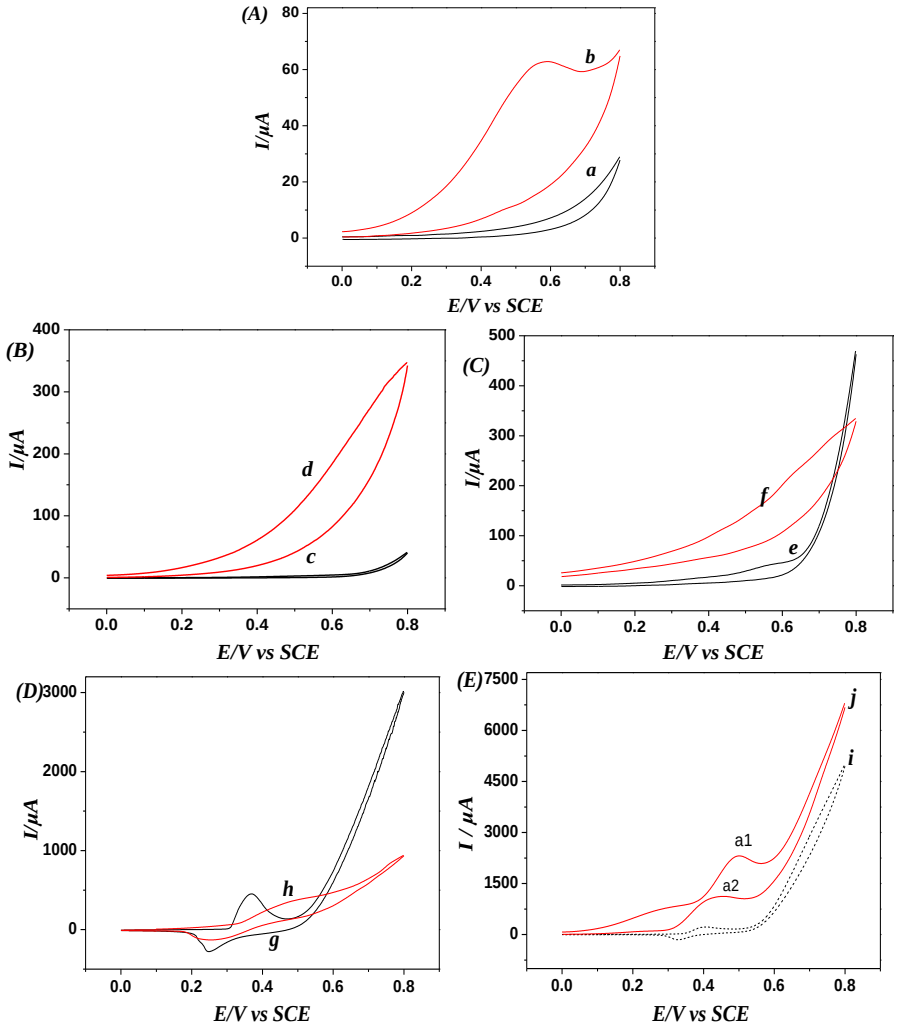

Figure 4. CVs of bare GCE (A), Graphite/GCE (B), NaY/GCE (C), Ni(II)Y/GCE (D), Ni(II)(salen)Y/GCE (E) in the absence (a, c, e, g, i) and the presence (b, d, f, h, j) of 0.075 M hydrazine hydrate in 1.0 M NaOH solution at scan rate of 20 mV s^{-1}.

$$Ni(II)(OH)_2(salen)+OH^- \underset{+e^-}{\overset{-e^-}{\rightleftharpoons}} Ni(III)(OOH)(salen)+H_2O \quad (E)$$

$$Ni^{III}(OOH)(Salen)+N_2H_4 \longrightarrow Ni^{II}(OH)_2(Salen)+product \quad (C')$$

Scheme 1. Electrocatalytic reaction mechanism for hydrazine at the surface of Ni(II)(salen)Y/GCE.

To confirm and get more about the electrocatalytic oxidation reaction mechanism, cyclic voltammetry and chronoamperometry were conducted. Fig.5 illustrates a series of cyclic voltammograms of Ni(II)(salen)Y/GCE at scan rate of 20 mV s^{-1} in 1.0 M NaOH solution containing different concentrations of hydrazine ranging in 0~0.25 M. As shown in Fig. 5, the anodic peak current enhances gradually with increase in hydrazine concentration, suggesting an interaction between the hydrazine and the film redox sites confined at the electrode surface. Inset (A) shows the magnification of the CVs of Fig.5 (curves a, c, e and g) in presence of 0, 0.01, 0.035 and 0.075 M hydrazine. As shown in inset (A), with potential scan to positive position, the first oxidation potential region (a1) with a significantly large peak current appears at potential above 0.499 V. At the reverse scan, no reduction peak is observed at the hydrazine concentration greater than 0.035 M but a new oxidation peak (a2) 50 mV lower than the potential of a1 peak is obtained, indicating that hydrazine is still oxidized in this potential region. This result suggests that chemical reaction rate between Ni(III)(OOH)(salen) and hydrazine increases with the concentration of hydrazine and is just right equal to the oxidation rate of Ni(II)$(OH)_2$(salen) to Ni(III)(OOH)(salen) at 0.035 M hydrazine.

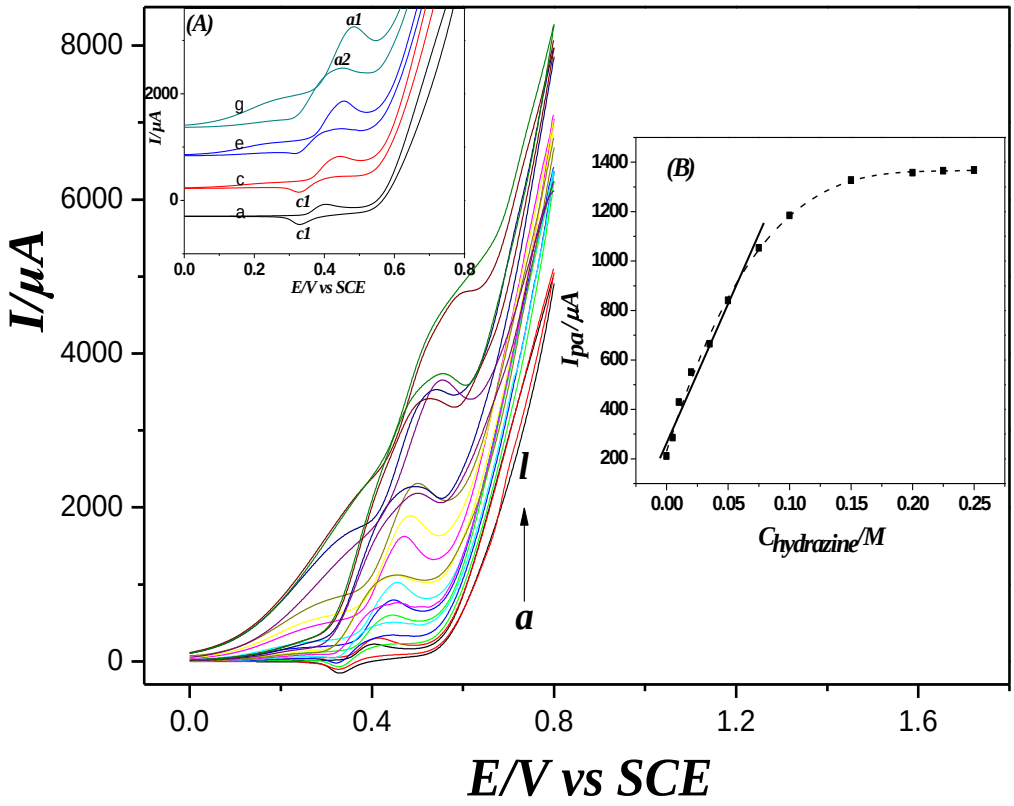

Figure 5. Cyclic voltammograms of Ni(II)(salen)Y/GCE at scan rate of 20 mV s^{-1} in 1.0 M NaOH solution containing different concentrations of hydrazine hydrate: (a) 0.00 M, (b) 0.005 M, (c) 0.01M, (d) 0.02M, (e) 0.035M, (f) 0.05 M, (g) 0.075 M, (h) 0.1 M, (i) 0.15 M, (j) 0.2 M, (k) 0.225 M, (l) 0.25 M; Inset (A): the magnification of curves a, c, e and g; Inset (B): plot of I_{pa} vs $C_{hydrazine}$.

This also leads to the second anodic peak a2, and the cathodic peak c1 decreases with the increase of concentration of hydrazine. In this process the Ni(III)(OOH)(salen) is reduced by hydrazine to Ni(II)$(OH)_2$(salen) and the resulting Ni(II)$(OH)_2$(salen) is further oxidized in the next circle of positive potential scan. So the catalytic oxidation circle of hydrazine, containing electrochemical reaction of Ni(III)(OOH)(salen)/Ni(II)$(OH)_2$(salen) (E) and chemical reaction (C'), is consistent with the mechanism of Scheme 1. Inset (B) of Fig. 5 illustrates the correlation between the anodic peak intensity and hydrazine concentration in the range of 0~0.25 M. As is obvious, the peak current is linear up to 0.075 M and then becomes plateaued at higher concentrations. This plot resembles a Langmuir-type plot [25, 40], potentially due to a Langmuir-type adsorption process (i.e., adsorption of hydrazine onto Ni(II)(salen)Y) that may influence electrocatalysis at the modified electrodes.

To get more information about kinetics of electrooxidation of hydrazine on the Ni(II)(salen)Y/GCE, the effect of scan rate on the electrocatalytic oxidation of hydrazine at the Ni(II)(salen)Y/GCE was also investigated by CV (Fig.6). As can be observed in Fig.6, the oxidation peak potential shifted to more positive potentials with increasing scan rate, confirming the kinetic limitation in the electrochemical reaction. Also, a plot (inset (a) in Fig. 6) of peak current versus the square root of scan rate is found to be linear in the range of 0.005-0.15 V s^{-1}, suggesting that, at sufficient overpotential, the reaction of hydrazine is controlled by the diffusion of hydrazine as well as kinetic process. In addition, with increasing scan rate, the catalytic oxidation peak potential (E_p) shifts to more positive values and there is a linear correlation between the peak potential and the logarithm of scan rate, log(v), as is illustrated in Fig. 6 (inset (b)). The Tafel slope b can be obtained from the linear relationship of E_p *vs* log(v) by using the following equation (3):

$$E_p = \frac{b}{2}\log v + cons\tan t \qquad (3)$$

On the basis of Eq. (3), the slope of E_p *vs* log(v) plot is $b/2$, where b indicates the Tafel slope. The plot of E_p *vs* log(v) indicates a linear variation for scan rates in the range of 5-60 mV s^{-1} (inset (b)). The slope is $E_p/\log v$, which is found to be 0.069 V in this work. So, $b = 2\times0.069 = 0.138$ V. Assuming the number of electrons transferred in the rate-limiting step is equal to one, a transfer coefficient, α, is estimated as 0.57. Also, the Tafel slope does not change in different hydrazine concentrations in 1.0 M NaOH, suggesting that a unique mechanism independent of hydrazine concentration operates, where the rate-determining step is the first electron transfer.

The total number of electrons (n) in the overall hydrazine oxidation reaction can also be obtained from the slope of I_p *vs* $v^{1/2}$ according to the following equation (4) for a totally irreversible diffusion controlled processes [22]:

$$I_p = 3.01\times10^5 n[(1-\alpha)n_\alpha]^{1/2} AC^* D^{1/2} v^{1/2} \qquad (4)$$

According to above result of Tafel slope, $(1-\alpha)n_\alpha$=0.43, geometric area (A) of 0.0707 cm^2 and D=3.47×10^{-7} cm^2 s^{-1}, as obtained by chronoamperometry (see below), C^* the bulk concentration of hydrazine (0.075 M), the value obtained for n is 4 (n=3.82). This implies that electrooxidation of hydrazine on the Ni(II)(salen)Y/GCE produces nitrogen and water. The calculated value of n=4 for the electrooxidation of hydrazine has been previously reported in the literatures [6, 21, 22].

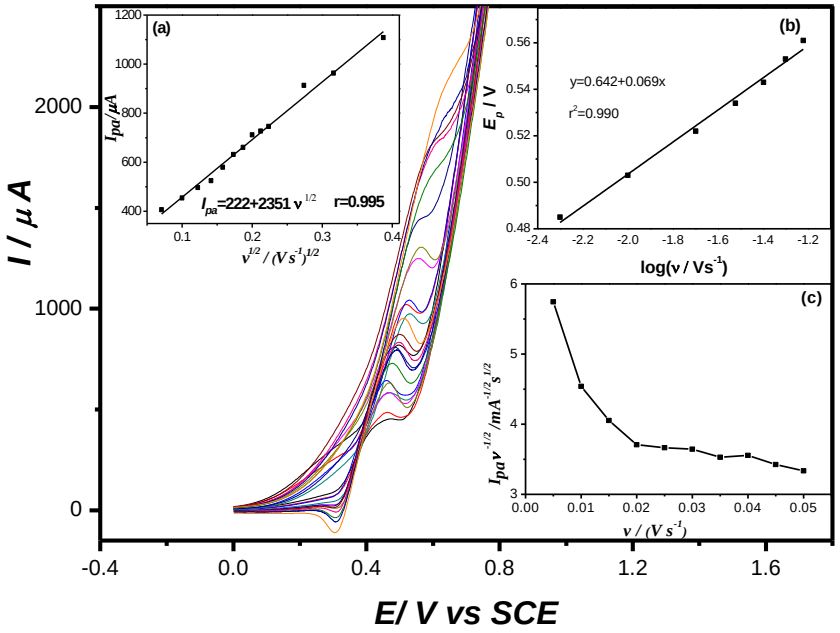

Figure 6. Cyclic voltammograms of Ni(II)(salen)Y/GCE in 1.0 M NaOH solution containing 0.075 M hydrazine hydrate at scan rates from a to p : 0.005, 0.01, 0.02, 0.03, 0.04, 0.05, 0.06, 0.07, 0.08, 0.09, 0.1, 0.15, 0.2, 0.3, 0.4, 0.5, 0.6, 0.7, 0.8, 0.9, 1V s^{-1}. Inset (a) plot of I_{pa}-$v^{1/2}$; (b) Tafel plot derived from the current-potential curve recorded at scan rate of 10 mV $s^{-1}$and (c) Variation of the scan rate normalized current (I_{pa}·$v^{-1/2}$) *vs* scan rate.

Furthermore, the plot of scan rate-normalized current ($I_pv^{-1/2}$) *vs* scan rate (inset (c) of Fig.6) also exhibits a characteristic shape typical of an EC' process [21], which complies with the above result as shown in scheme 1. Also, it can be found that the cathodic peak current increases with scan rate because there is not enough time at high scan rate for the catalytic reaction between hydrazine and Ni(III)(salen)Y, some of which is then reduced at reversal scan. On the basis of this study and that reported in literature [6], the following mechanism can be proposed for the oxidation of hydrazine on the Ni(II)(salen)Y/GCE in alkaline solutions, considering that hydrazine presents in its unprotonated form in alkaline solutions:

$N_2H_4 + OH^- \longrightarrow N_2H_3 + H_2O + e^-$ (slow) (5)

$N_2H_3 + 3OH^- \longrightarrow N_2 + 3H_2O + 3e^-$ (fast) (6)

The rate-determining step is one electron transfer followed by a 3-electron process to give N_2 as a final product. The general reaction mechanism of hydrazine oxidation catalyzed by the Ni(salen)Y catalyst can be expressed as scheme 2:

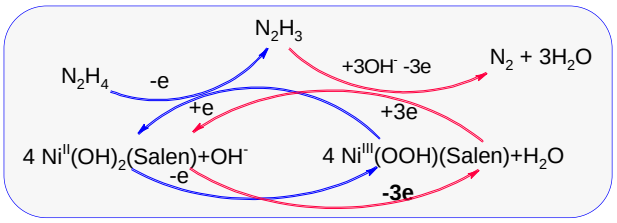

Scheme 2. The sketch of the general reaction mechanism for hydrazine catalytic oxidation

So the overall reaction equation can be expressed as following reaction (7), showing that hydrazine oxidation on the Ni(salen)Y/GCE produces nitrogen and water.

$$N_2H_4 + 4OH^- \longrightarrow N_2 + 4H_2O + 4e^- \quad (7)$$

3.3. Chronoamperometric measurements

Chronoamperometric measurements of hydrazine at Ni(II)(salen)Y/GCE were carried out in different concentration of hydrazine and used for evaluation of the diffusion coefficient, *D*, of hydrazine (shown as Fig. 7). The chronoamperograms in Fig. 7 show that an increase in hydrazine concentration is accompanied by an increase in anodic currents obtained at a potential of 500 mV versus SCE. For an electroactive material (hydrazine in this case) with a diffusion coefficient of *D*, the current observed for the electrochemical reaction at the mass transport limited condition is described by the Cottrell equation (8)[24]:

$$I = nFAD^{1/2}C^{*}\pi^{-1/2}t^{-1/2} \quad (8)$$

Based on the Cottrell equation (8), the experimental plot of I vs $t^{-1/2}$ is linear as described in inset (a) of Fig. 7 with hydrazine concentrations of 0.01, 0.02, 0.035, 0.05 and 0.075 M. The slopes of the resulting straight lines are plotted versus hydrazine concentration (inset (b) of Fig. 7). From the resulting slope and Cottrell equation the mean value of D is found to be 3.47×10^{-7}cm^2/s. This value of diffusion coefficient is lower than 3.8×10^{-6} cm^2/s [22], 4.5×10^{-6} cm^2/s [27], 1.1×10^{-6} cm^2/s [23] that were reported in the literatures.

Chronoamperometry can also be used for evaluation of the catalytic rate constant, k_{cat}, for the reaction between hydrazine and the Ni(II)(salen)Y/GCE according to the method of Zheng and Song [24]. At intermediate time, when the oxidation current is dominated by the rate of the electrocatalytic reaction of hydrazine, the catalytic current I_{cat} could be written as follows (9):

$$\frac{I_{cat}}{I_L} = \pi^{1/2}(k_{cat}c_0t)^{1/2} \quad (9)$$

where I_{cat} and I_L are the currents in the presence and the absence of hydrazine, respectively. k_{cat} the catalytic rate constant ($M^{-1}s^{-1}$), c_0 the bulk concentration (M) of hydrazine and t the time elapsed (s). So, k_{cat} of the heterogeneous catalytic reaction between hydrazine and redox sites in the Ni(II)(salen)Y modified electrode (namely heterogeneous rate constant) can be obtained from the slope of I_{cat}/I_L vs $t^{1/2}$ (Fig. 8) at a given hydrazine concentration. From the value of the slope, k_{cat} is found to be 1.54×10^5 $M^{-1}s^{-1}$ for 0.02M hydrazine, which is higher than those reported previously [23]. Table 1 compares the results of this work with those reported by others [21, 23, 24, 27]. As shown in table 1, the catalytic rate constant of hydrazine oxidation on the Ni(II)(salen)Y/GCE in this work is larger than those reported in the literatures [21, 23, 24, 27], this is probably because the Ni(II)(salen)Y/GCE as the electron transfer media has inherently higher apparent electron transfer rate constant (k_s) exhibiting good electrochemical property although the diffusion coefficient (D) of hydrazine is small on the surface of Ni(II)(salen)Y modified electrode in alkaline solution.

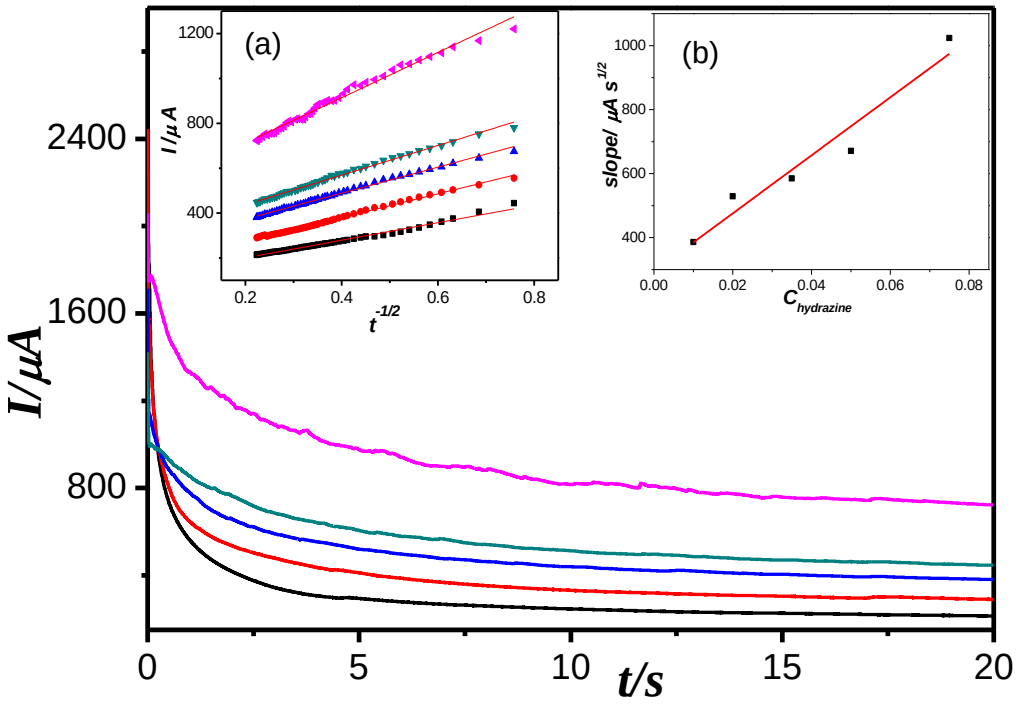

Figure 7. Chronoamperograms response of Ni(II)(salen)Y/GCE in 1.0 M NaOH solution containing 0.01, 0.02, 0.035, 0.05 and 0.075 M hydrazine at potential of 500 mV vs SCE.

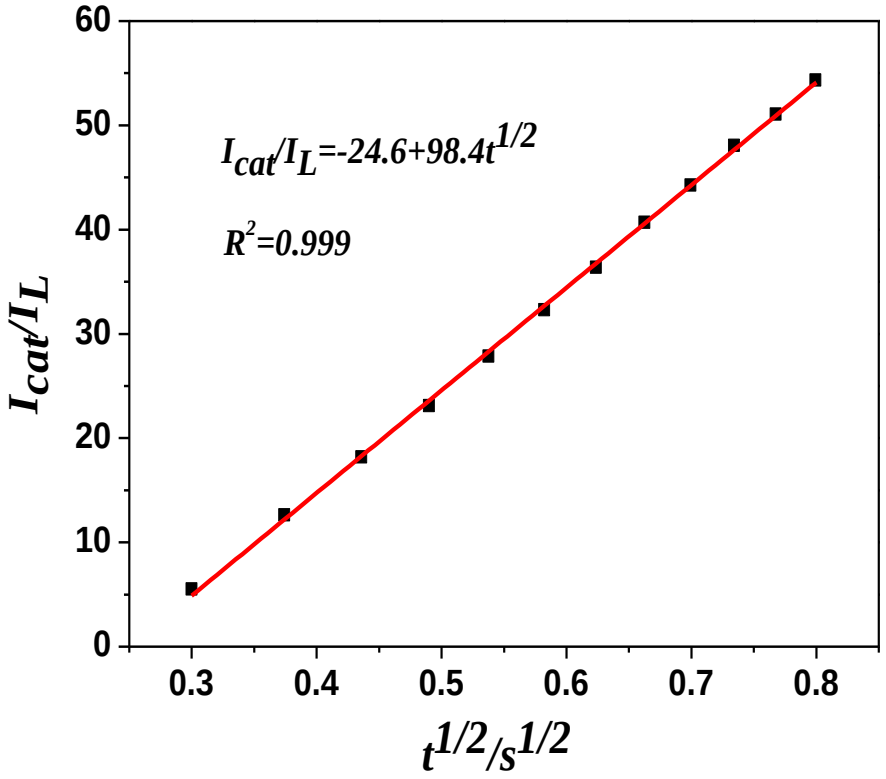

Figure 8. Plot of I_{cat}/I_L vs $t^{1/2}$ on Ni(II)(salen)Y/GCE in 1.0 M NaOH solution of 0.02 M hydrazine.

Table 1. Comparison of some of the characteristics of hydrazine oxidation at different modified electrodes

parameters	Ref. [21]	Ref. [27]	Ref. [24]	Ref. [23]	This work
The apparent electron transfer rate constant (k_s/s^{-1})	0.51	1.5	2.21	4.44	7.74
Heterogeneous rate constant between hydrazine and Ni(II)(salen)Y/GCE (k_{cat}/M^{-1} s^{-1})	3.95×10^{4}	-	4.78×10^{4}	4.83×10^{3}	1.54×10^{5}
Electron transfer coefficient between hydrazine and Ni(II)(salen)Y/GCE (α)	0.45	0.47	-	0.35	0.57
Diffusion coefficient (D/cm^2 s^{-1})	1.1×10^{-5}	4.5×10^{-6}	3.58×10^{-5}	1.1×10^{-6}	3.47×10^{-7}

4. CONCLUSIONS

In summary, a kind of Y-type zeolite encapsulated Ni(II)(salen) (Ni(II)(salen)Y) catalyst was synthesized and characterized successfully. The Ni(II)(salen)Y was applied for modification the glass carbon electrode. Cyclic voltammetry results showed that the modified electrode had a good catalytic effect towards electrooxidation of hydrazine in pH=14 alkaline media. The electrooxidation of hydrazine on the Ni(II)(salen)Y/GCE was found to be a diffusion-controlled electrocatalytic process in a wide potential range, which proceeds via (EC') mechanism. The diffusion coefficient (D) and catalytic rate constant (k_{cat}) of hydrazine are obtained according to diffusion controlled hydrazine oxidation reaction on the Ni(II)(salen)Y/GCE. Furthermore, the general reaction mechanism for the oxidation of hydrazine on the Ni(II)(salen)Y/GCE in alkaline solutions is proposed and found to be the first electron transfer reaction as the rate-limiting step followed by a 3-electron process to produce environmentally friendly nitrogen and water as final products.

ACKNOWLEDGEMENT
This work was supported by the Shanxi Provence Natural Science Foundation in China (No. 2013011012-1)

References

1. R. Liu, X. Jiang, F. Guo, N. Shi, J. Yin, G. Wang and D. Cao, *Electrochim. Acta*, 94 (2013) 214
2. E.H. Vernot, J.D. MacEwen, R.H. Bruner, C.C. Haus and E.R. Kinkead, *Fund Appl. Toxicol.*, 5 (1985) 1050
3. M.R. Andrew, W.J. Gressler, J.K. Johnson, R.T. Short and K.R. Williams, *J. Appl. Electrochem.*, 2 (1972) 327
4. V. Rosca and M.T.M. Koper, *Electrochim. Acta*, 53 (2008) 5199
5. A. Serov and C. Kwak, *Appl. Catal. B Environ.*, 98 (2010) 1
6. M. Hosseini, M.M. Momeni and M. Faraji, *J. Mol. Catal. A Chem.*, 335(2011) 199
7. F. Gholamian, M. A. Sheikh-Mohseni and H. Naeimi, *Mater. Sci. & Eng., C* 32(2012) 2344

8. H. Hosseini, H. Ahmar, A. Dehghani, A. Bagheri, A.R. Fakhari and M. Mostafa Amini, *Electrochim. Acta*, 88 (2013) 301
9. L. Tamašauskaitė-Tamašiūnaitė, J. Rakauskas, A. Balčiūnaitė, A. Zabielaitė, J. Vaičiūnienė, A. Selskis, R. Juškėnas, V. Pakštas and E. Norkus, *J. Power Sources,* 272 (2014) 362
10. R. Madhu, V. Veeramani and S-M. Chen, *Sensors and Actuators B*, 204 (2014) 382
11. K. Ghanbari, *Synthetic Met.*, 195 (2014) 234
12. G. Gao, D. Guo, C. Wang and H. Li, *Electrochem. Commun.*, 9 (2007) 1582
13. W.X. Yin, Z.P. Li, J.K. Zhu and H.Y. Qin, *J. Power Sources*, 182 (2008) 520
14. V. Rosca and M.T.M. Koper, *Electrochim. Acta,* 51(2008) 5399
15. K. Yamada, K. Yasuda, H. Tanaka, Y. Miyazaki and T. Kobayashi, *J. Power Sources*, 122 (2003) 132
16. K. Yamada, K. Asazawa, K. Yasuda, T. Ioroi, H. Tanaka, Y. Miyazaki and T. Kobayashi, *J Power Sources*, 11(2003) 5236
17. L. Zhang, W. Niu, W. Gao, L. Qi, J. Zhao, M. Xu and G. Xu, *Electrochem. Commun.*, 37 (2013) 57
18. L. Chen, G. Hu, G. Zou, S. Shao and X. Wang, *Electrochem. Commun.*, 11 (2009) 504
19. H. Lin, J. Yang, J. Liu, Y. Huang, J. Xiao and X. Zhang, *Electrochim. Acta.*, 90 (2013) 382
20. K. Asazawa, K. Yamada, H. Tanaka, A. Oka, M. Taniguchi and T. Kobayashi, *Angew Chem Int Ed*, 46 (2007) 8024
21. M. Mazloum-Ardakani and A. Khoshroo, *Electrochim. Acta*, 103 (2013) 77
22. H. R. Zare, M.R. Shishehbore, D. Nematollahi and M. S. Tehrani, *Sensors and Actuators B*, 151 (2010) 153
23. M.M. Ardakani, P.E. Karami, P. Rahimi, H.R. Zare and H. Naeimi, *Electrochim. Acta,* 52 (2007) 6118
24. L. Zheng and J.F. Song, *Talanta,* 79 (2009) 319
25. U.P. Azad and V. Ganesan, *Electrochim. Acta* 56 (2011) 5766
26. M. Ebadi, *Can. J. Chem.*, 81(2003) 161
27. A. Benvidi, P. Kakoolaki, H.R. Zare and R. Vafazadeh, *Electrochim. Acta,* 56 (2011) 2045
28. M.A. Kamyabi, O. Narimani and H.H. Monfared, *J. Electroanal. Chem.*, 644 (2010) 67
29. R. Zhang, J. Ma, W. Wang and R. Li, *J. Electroanal. Chem.*, 643 (2010) 31
30. R. Zhang, W. Zhang, L. Gao, J. Zhang, P. Li, W. Wang and R. Li, *Appl Catal A Gen*, 466 (2013) 264
31. M.F.S. Teixeira, M.F. Bergamini, C.M.P. Marques and N. Bocchi, *Talanta,* 63 (2004) 1083
32. T. Rohani and M.A. Taher, *Talanta*, 78 (2009) 743
33. A. Babaei, M. Zendehdel, B. Khalilzadeh and A Taheri, *Colloids Surf B*, 66 (2008) 226
34. J.B. Raoof, N. Azizi, R. Ojani, S. Ghodrati, M. Abrishamkar and F. Chekin, *Int. J. Hydrogen Energy*, 36 (2011) 13295
35. P.V. Samant and J.B. Ferndes, *J. Power Sources*, 125 (2004) 172
36. A. Zimmer, D. Monter and W. Reschetilovski, *J. Appl. Electrochem.*, 33 (2003) 933
37. B. Fan, H. Li, W. Fan, C. Jin and R. Li, *Appl. Catal. A Gen.* 340 (2008) 67
38. R. Raja and P. Ratnasamy, *J. Catal.* 170 (1997) 244
39. C. Jin, W. Fan, Y. Jia, B. Fan, J. Ma and R. Li, *J. Mol. Catal. A*, 249 (2006) 23
40. M. Pal and V. Ganesan, *Analyst*, 135 (2010) 2711